ГЛОБАЛЬНАЯ ЯДЕРНАЯ БЕЗОПАСНОСТЬ, 2016 №1(18), С. 34–45

ИЗЫСКАНИЕ, ПРОЕКТИРОВАНИЕ, СТРОИТЕЛЬСТВО И МОНТАЖ ТЕХНОЛОГИЧЕСКОГО ОБОРУДОВАНИЯ ОБЪЕКТОВ АТОМНОЙ ОТРАСЛИ

УДК 621.791.725

ЛАЗЕРНАЯ И ГИБРИДНАЯ ЛАЗЕРНО-ДУГОВАЯ СВАРКА ХЛАДОСТОЙКИХ СТАЛЕЙ С СОДЕРЖАНИЕМ НИКЕЛЯ ДО 9%

© 2016 С.Э. Гоок*, А.В. Гуменюк*,, М. Ретмайер*,**, А.М. Эль-Батаги*****

** Общество Фраунгофера,*
Институт производственных систем и технологий конструирования ИПК, Берлин, Германия
*** Федеральное ведомство по исследованию и испытаниям материалов БАМ, Берлин, Германия*
**** Центральный металлургический научно-исследовательский институт, Хелуан, Египет*

Термообработанные конструкционные хладостойкие стали с содержанием никеля до 9% считаются наиболее подходящим по своим стоимостным показателям материалом для изготовления элементов криогенных систем в различных сегментах энергетического машиностроения. Данный тип сталей характеризуется высокими прочностными показателями в сочетании с высокими значениями ударной вязкости при температурах эксплуатации до -196 ^{0}C. Для сварки хладостойких никельсодержащих сталей рекомендованы, и в настоящее время широко используются присадочные материалы на основе никеля. Основной проблемой этого выбора является снижение предела текучести металла сварного шва, которое компенсируется за счет увеличения толщины стенки изделия. Присадочные материалы на никелевой основе относительно дороги и необходимы в большом количестве для заполнения разделок под многопроходную сварку. Эти факторы значительно увеличивают затраты при изготовлении крупногабаритных толстостенных изделий, как например резервуаров для хранения сжиженного природного газа. По этим причинам, освоение новых сварочных технологий представляет большой экономический интерес. Значительный потенциал предлагают методы сварки, основанные на применении современных высокомощных оптоволоконных лазеров. Лазерный луч приводит к возникновению гораздо меньшей зоны плавления по сравнению с традиционными, дуговыми процессами. При этом уменьшается тепловая нагрузка на основной металл. Металл шва по своему химическому составу и прочностным свойствам приближается к основному металлу. Форма разделки под лазерную сварку толстостенных изделий подразумевает наличие высокого притупления проплавляемого за один проход, что позволяет значительно сократить количество присадочного материала, необходимого для заполнения разделки. До настоящего времени подробные исследования относительно применения лазерных технологий для сварки хладостойкой никельсодержащей стали не были проведены.

В настоящей работе рассмотрены особенности формирования сварного шва при лазерной и гибридной лазерно-дуговой сварке листов хладостойкой никельсодержащей стали толщиной 11,5 мм. Рекомендованы параметры процесса, обеспечивающие стабильное проплавление стыка и равномерное формирование корня шва. С помощью электронно-зондового микроанализа определена глубина проникновения и исследован характер распределения присадочной проволоки в узком гибридном лазерно-дуговом шве. Испытания на разрыв не выявили снижения прочностных свойств как лазерных, так и гибридных лазерно-дуговых швов. Разрушение испытанных образцов происходит по основному металлу вдали от сварного шва.

Ключевые слова: хладостойкие стали, никельсодержащие стали, лазерная сварка, перемешивание, предел прочности.

Поступила в редакцию 18.03.2016 г.

INTRODUCTION

As the world searches for cleaner energy sources, one that shows great promise now and in the years to come is natural gas. Burning cleaner than oil, and much cleaner than coal as well as being abundant, natural gas is an obvious choice to meet the worlds increasing energy needs while meeting increasingly tight restrictions on CO_2 [1, 2, 3]. Natural gas resources are typically located away from the areas of consumption, making transportation and storage of large quantities of natural gas necessary. Storage and transportation of natural gas can be done more efficiently when it is cooled below -165°C and liquefied. The reason for this step is LNG takes up $1/600^{th}$ the volume compared to natural gas at room temperature.

LNG is stored in large, specifically designed underground or aboveground cryogenic storage containers. The aboveground, flat-bottomed, cylindrical LNG tank design is more commonly used throughout the world [4, 5]. The typical cryogenic storage containers are comprised of an inner and an outer shell. The inner shell, so-called primary container, is made from cryogenic steel enclosed in the outer shell, made either from carbon steel or pre-stressed concrete.

Over the last 20 years aboveground storage tank capacities have grown in size by a factor of two. With capacities of 80.000 m^3 in the 80's the capacities of 140.000-160.000 m^3 are now common, and trending to capacities up to 200.000 m^3. The inner shell of such large tank has a diameter of 84 m and a height of 38 m and is constructed from many 9%Ni steel sheets that are welded together. To reach this tank capacity, plates that are 50 mm thick are required. The length of welds totals to roughly 3200 m.

Heat treated 9%Ni steel exhibits superior mechanical properties at operating temperatures at a reasonable price and is commonly used for the construction of inner shells of LNG storage tanks. The excellent low temperature impact toughness of tempered 9%Ni steel is the result of a fine grained structure of tough nickel-ferrite with small amounts of stable austenite formed by tempering [6, 7]. Ni based welding consumables is the preferred filler material of choice in LNG tank construction [6, 8, 9].

Currently most welds during the construction of LNG tanks are preformed using conventional arc welding processes, i.e. shielded metal arc welding (SMAW), gas metal arc welding (GMAW), gas tungsten arc welding (GTAW) and submerged arc welding (SAW) [10]. Ni based filler materials have great resistance to brittle failure at operating temperature (-165 °C) and hence have provided excellent safety record for LNG tanks. The high resistance to brittle failure results in a filler metal with lower strength than the base metal (BM). The design codes compensate for this lack of strength by increasing the thickness of the tank wall to ensure the welds do not fail.

Typical groove configuration for SMAW, GTAW and SAW used for joining 9%Ni steel plates is double sided groove with an beveling angle at about 60°. The filling of such welds using conventional welding methods is time consuming and requires a large amount of expensive filler material. Industry has expressed interest in looking for ways to increase the speed of production and reduce the amount of material needed for the construction of LNG tanks. Some obvious places to start looking to reduce the cost/time of production are in the welds. Options include creating stronger welds to increase the maximum allowable stress in the wall material, utilizing less expensive filler material, creating joint geometry that requires less filler material and less welding passes and using faster joining processes. For these reasons new welding technologies are the focus of interest. Big potential can be seen in laser based welding techniques.

Autogenous laser welding provides deep penetrating welds. It is much faster than manual arc techniques and can be easily automated. However, laser welding is not without drawbacks; one of them is the need for near perfect part fit-up which is not always possible. This limitation arises due to the small diameter of laser beam, which is (depending on laser

source and focusing optic) about 0.4 – 0.5 mm in the focal plane. Gap sizes above this limit are difficult to bridge. Lack of fusion is a typical weld imperfection in oversized gaps. High precision in the positioning of the laser beam to the joint is needed. The second drawback of autogenous laser welding is the short thermal cycle and the associated high cooling rate. For high strength steels, which include cryogenic 9%Ni steel and others that are common to the oil and gas industry, these fast cooling rates can lead to the formation of unfavorable hard and brittle martensitic microstructure. Martensite has detrimental effects on the mechanical properties of the steel; reducing ductility, fatigue life and fracture toughness.

A solution to this issue of tight tolerances on part fit up can be slightly alleviated by the addition of filler material. Welding wire can be added to the molten pool either with an arc or in a cold wire configuration. Hybrid laser-arc welding (HLAW) and laser cold wire welding are quite well known welding processes. They are robust and therefore worth considering for the welding of thick walled constructions, for example LNG tanks.

A certain concentration of filler material in the fusion zone (FZ) is needed in order to improve the mechanical properties of the weld joint. Laser welds have a thin deep FZ profile. The transportation of filler material in the depth of these thin laser welds is a technical challenge. Recent studies have shown that the maximum penetration depth of filler material by hybrid laser-arc welding is limited to 13 … 15 mm [11, 12]. It has to be mentioned that the distribution of the wire feeding elements becomes very inhomogeneous starting at roughly 4 mm from the top side of the weld. It is unclear if such distribution of alloying elements is adequate to aid in the recovery of mechanical properties in the weld joint. The question regarding the necessary percentage of Ni to achieve the required toughness for LNG tanks is of a big practical interest.

In the frame of this study trials of HLAW and laser cold-wire welds were compared to laser only welds. Peculiarities of welding process stability and weld formation were documented and analyzed. The focus of welding trials was also the maximizing the filler wire penetration depth without causing cracks. Using EPMA of %Ni, hardness mapping and optical microscopy the effectiveness of hybrid verses cold-wire laser welding regarding the achievable mechanical characteristics of the welds was determined.

1. EXPERIMENTAL

A fiber laser YLR-20000 (IPG) with max power output of 20 kW and beam parameter product (BPP) of 11.5 mm x mrad supplied the laser power through a fiber optic cable with a core diameter of 200 µm. Laser optics BIMO-HP (HIGHYAG) was used to focus the beam to a spot size of 0.5 mm with a focal length of 350 mm. The arc and filler wire was supplied via a Qineo Pulse 600 (CLOOS) power supply. Welding process arrangements are shown in Figure 1.

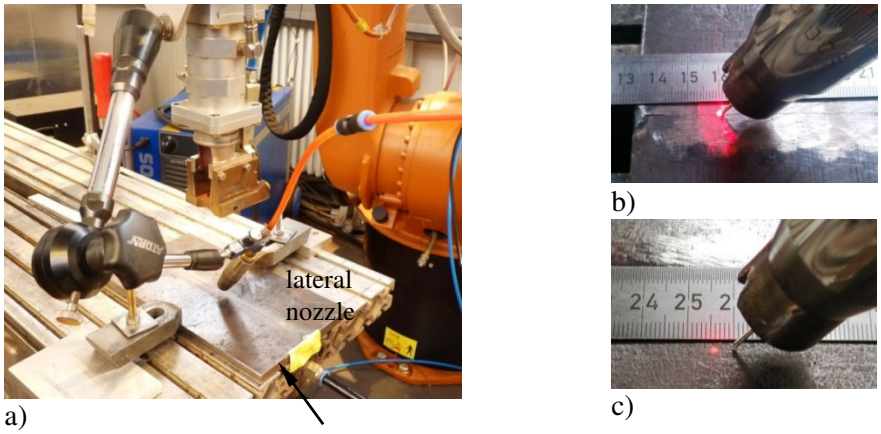

Figure 1 – Welding process arrangements; laser welding (a); laser cold wire welding (b); hybrid laser-arc welding (c)

Top side shielding gas was adjusted from pure Ar in laser only and laser cold wire welding, to Ar+30%He for hybrid laser-arc welding to help with arc stability. In the case of laser welding the shielding gas has been supplied through the lateral nozzle (Figure 1a). A GMA-torch was mounted on the optics to provide hybrid as well as cold wire process. The angle between GMA-Torch and laser beam axis was 25°. The distance between laser beam and wire tip for the laser cold wire was zero (Figure 1b) and for the hybrid process it was between 4 mm and 5 mm (Figure 1c). The HLAW process was performed in leading arc configuration.

European Standard EN10028-4 was followed for the selection of the materials for these experiments. The base material was X8Ni9, its exact composition was determined by Optical Emission Spectrometer (OES) and is displayed in Table 1. Notably the Ni content for the selected base metal falls within the standards acceptable range of 8.5-10.0 wt%. The filler material has been chosen according to recommendation DVS 0955 [9]. The composition of Ni-based filler wire Thermanit 625 (ERNiCrMo-3) is also in Table 1. The filler wire and base metal have very similar mechanical properties (Table 2). However one notable difference is the higher tensile strength of the filler wire, achieved through alloying of Molybdenum and Chromium.

Table 1 – Composition of materials used, shown in wt%

Material / Element	C	Si	Mn	P	S	Cr	Ni	Cu	Mo	Nb	Fe
X8Ni9 (BAM analysis)	0.05	0.22	0.52	0.006	0.002	0.02	8.8	0.05	0.01	0.01	>90
Thermanit 625	0.03	0.25	0.2	-	-	22.0	bal.	-	9.0	3.6	<1.0

Table 2 Mechanical properties of materials used (reference values)

Material	Yield strength in MPa (min)	Tensile strength in MPa (min)	Charpy value at -196°C in J	
			Transverse	Longitudinal
X8Ni9 (normalized base metal)	490	640	40	50
Thermanit 625	460	740	40	

Welding specimen preparation included cutting the base material to 80 mm x 250 mm x 11.5 mm sheets with mille edges. The plates were then tacked with no gap nor misalignment. The root side was shielded with pure Ar and a focus position Δz of 3 mm below plate surface was used for all welds preformed. Welding parameters can be seen in Table 3.

Table 3 Welding parameters

Welding parameter / Process	Laser	Laser cold wire	Laser hybrid
Laser power in kW	12.7 … 13.8	13 … 15	11 … 13
Welding speed in m/min	1.5 … 2	2	1.8 … 3
Peak arc current in A	-	-	365
Peak arc voltage in V	-	-	35
Wire feed speed in m/min	-	2 … 2.5	5 … 12
Wire diameter in mm	-	1.2	1.2

2. RESULTS AND DISCUSSION

Series of welds have been performed with all three welding techniques. Parameter variation in the ranges given in Table 3 was used to achieve stable and reproducible welds with the best surface and root quality possible. Selected welds have been subjected to extensive metallographic examinations and mechanical-technological tests. X-ray examinations were made on most welds. No crack-like defects could be detected within the range of X-ray resolution.

2.1 Weld seam formation and microstructure

Autogenous laser welding

Recommended parameters for autogenous laser beam welding for 11.5 mm thick X8Ni9 is a laser power at 13.8 kW with welding speed of 2 m/min. The result is the crack free weld with abot 1 mm undercutting on the top side due to the material vaporization and spattering. The narrow FZ (~1–2 mm wide) is characteristic for such deep penetrated autogenous laser welds operating in keyhole mode. A macrograph of a laser only weld cross section is displayed in Figure 2a. The heat affected zone (HAZ) is also very narrow due to the high energy density of this welding process. Figure 2b shows the fusion boundary. Figure 2c is the FZ at higher magnification. The rolling direction is visible up to the fusion boundary where the weld metal (WM) microstructure becomes present, as seen in part b) of Figure 2. Weld metal microstructure of the autogenous laser weld is comprised of mostly untempered martensite with some ferrite throughout.

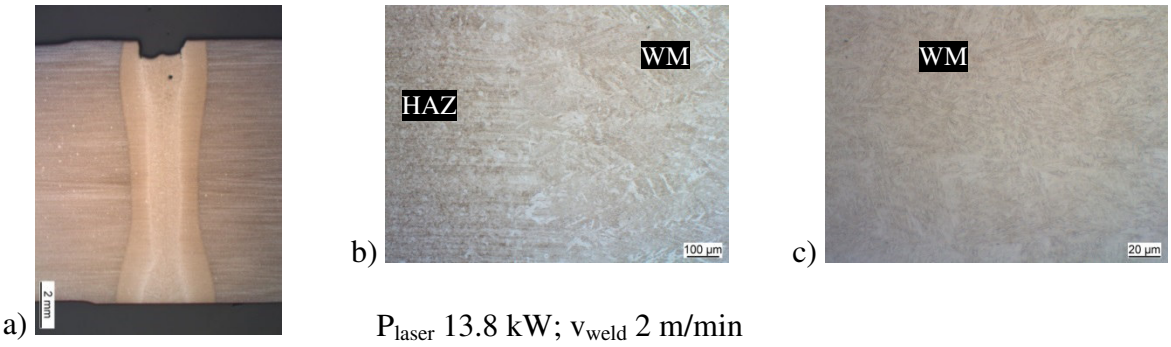

Figure 2 – Autogenous laser weld (a), varying magnifications of the same weld with focus on the fusion boundary (b) and weld metal (c)

Laser cold wire welding

The welding process has been adjusted so that the feeding wire was fed into the laser beam about 1 mm above the specimen surface and melted, then the molten wire metal was moved down to the keyhole under the force of gravity (Figure 3). The result was a well-shaped weld with minimal undercutting on the top-side and the excess weld material on the root-side (Figure 4a). Recommended parameters for laser cold wire welding is a laser power at 14 kW, welding speed of 2 m/min with a wire feeding speed of 2 m/min as well. An increasing of the wire feeding speed up to 2.5 m/min resulted in unstable wire melt-off due to the increase in relative speed between wire and specimen surface. The angle between the wire axis and specimen surface was 75°, what is quite steep. The rather unfavorable wire feeding angle in combination with the higher relative speed caused the wire to stumble on the cold specimen surface and deflected out of the laser beam path. Un-melted pieces of welding wire were frozen on the top of the weld and could be observed on the weld surface (red ovals in Figure 4b).

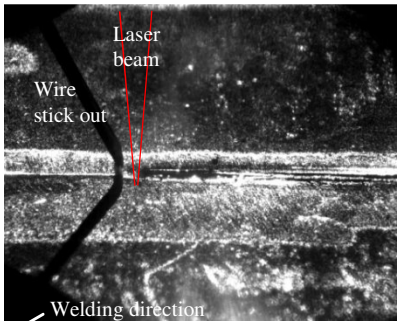

Figure 3 – Laser cold wire welding process observed with high speed camera

a) P_{laser} 14 kW; v_{weld} 2 m/min; v_{wire} 2 m/min

b) P_{laser} 14 kW; v_{weld} 2 m/min; v_{wire} 2.5 m/min

Figure 4 – Outer appearance of laser cold wire welds; with 2 m/min wire feeding speed (a); with 2.5 m/min wire feeding speed (b)

In the macrograph (Figure 5a) the general shape and dimensions of the laser cold wire weld are comparable to the laser only weld (Figure 2a). A more careful analysis will reveal the Ni rich filler material (white regions) to be penetrating to a depth of ~6 mm from the top of the weld, although the character of the dilution is very inhomogeneous.

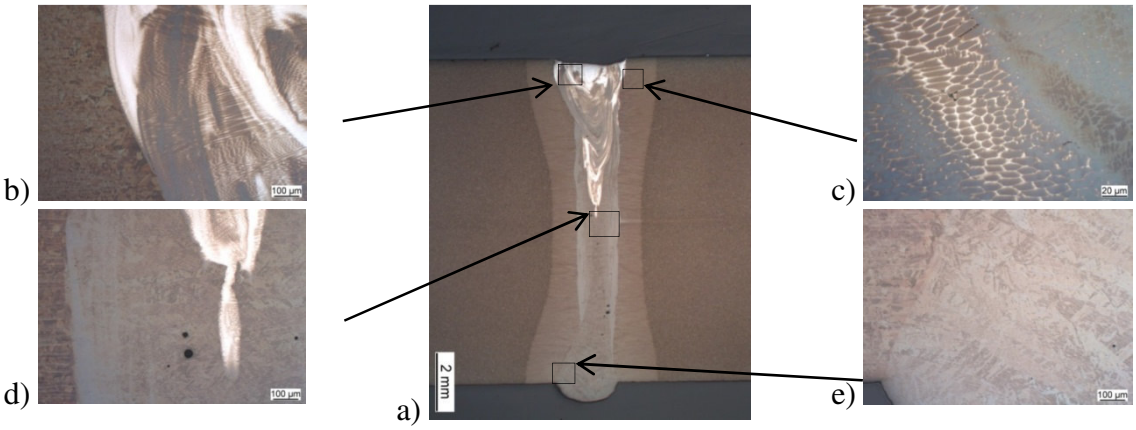

Figure 5 – Cold wire laser weld (P_{laser} 14 kW; v_{weld} 2 m/min; v_{wire} 2 m/min), varying magnifications with focus on the fusion boundary and FZ: general shape (a); top part (b, c); middle (d) and root part (e)

The fusion boundary of the top side is shown (Figure 5b). There are noticeable Ni rich areas of mixing. These areas are band-like in morphology and give evidence to the turbulent movement of the molten metal in the weld pool during the welding. Figure 5c displays the cellular dendritic solidification of the Ni rich areas. Austenitic structure is quite prominent in the top part of the weld. The penetration pattern becomes narrow and stops abruptly at the middle of the plate thickness (Figure 5d). Some porosity with a maximum pore diameter 50 µm is visible. Such discontinuities are subcritical and acceptable in the welding code for LNG tanks. The presence of filler material at the bottom side of the weld could not be detected by visual observation. The microstructure at the root side of the weld is martensite and ferrite (Figure 5e). Further quantifying details to the distribution of feeding wire alloying elements in the weld cross section will be given in the next section.

Hybrid laser-arc weld

The main problem at the hybrid laser arc welding of the 9%Ni steel was the formation of the excessive root with frozen droplets, so called root humping (Figure 6a). This phenomenon occurs due to the higher viscosity of molten Ni based wire used. The options for influencing the root humping were to reduce the arc pressure on the molten pool or to increase the traveling speed to avoid droplets formation. An appropriate weld root could be achieved at quite low wire feeding speed 5 m/min, welding speed 2.0 m/min and laser power 12.6 kW. The slight arc pressure on the top side of the weld in this case was not able to press the molten metal out of the weld root. The result was a stable weld without excessive root droplets

(Figure 6b). However, it is questionable if this technique is robust enough to be used in practice. The wire feeding speed was too low, not enough filler material was feed into the process and the arc transfer mode tended to be globular. A better way to stabilize the process was an increase of welding speed from 2 m/min to about 3 m/min and increasing laser power from 12.6 kW to about 14 kW. The wire feeding speed was held at 12 m/min, a typical speed for HLAW. Subsequently it was possible to produce a series of welds with an appropriate root quality. An example for the weld with increased welding speed is shown in Figure 6c.

a) P_{laser} = 12.6 kW,
v_{weld} = 2.0 m/min,
v_{wire} = 12 m/min,
I = 330 A, U = 33 V
b) P_{laser} = 12.6 kW,
v_{weld} = 2.0 m/min,
v_{wire} = 5 m/min,
I = 141 A, U = 26 V
c) P_{laser} = 13.8 kW,
v_{weld} = 3.0 m/min,
v_{wire} = 12 m/min,
I = 330 A, U = 33 V

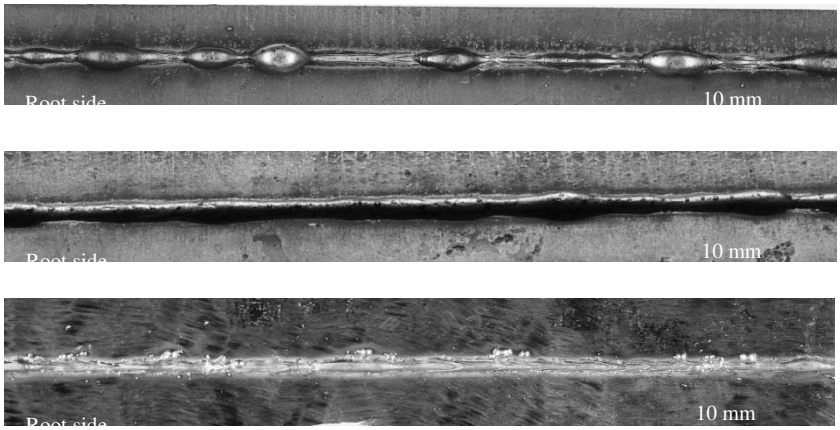

Figure 6 – Outer appearances of hybrid laser-arc welds (root side) performed with different welding parameters; weld without parameter adaptation (a); decreased welding wire feeding speed (b); increased welding speed and laser power (c)

Figure 7a shows the general view of the cross section for the HLAW weld performed with optimized parameters. The first noticeable difference from the laser and cold-wire welds is the shape of the FZ. Two distinct zones can be recognized: the wide FZ at the top of the weld and the narrow deep zone that penetrates material to underside. They can be defined as an arc dominated and a laser dominated zones. There are differences in the microstructure between the two zones. The arc dominated zone reaches about 4 mm in the depth and consists predominantly of austenite due to the austenitic filler material (Figure 7b and 7c). The filler material can be visually seen mixing to a weld depth of roughly 5 mm. After this depth level the dilution becomes extremely inhomogeneous. At 6 mm from the top (Figure 7d) solidification cracking is shown in the “islands” with high filler wire concentration. No presence of the filler material could be found by optical observation in the root of the weld. The microstructure of the weld root is ferritic-martensitic (Figure 7e).

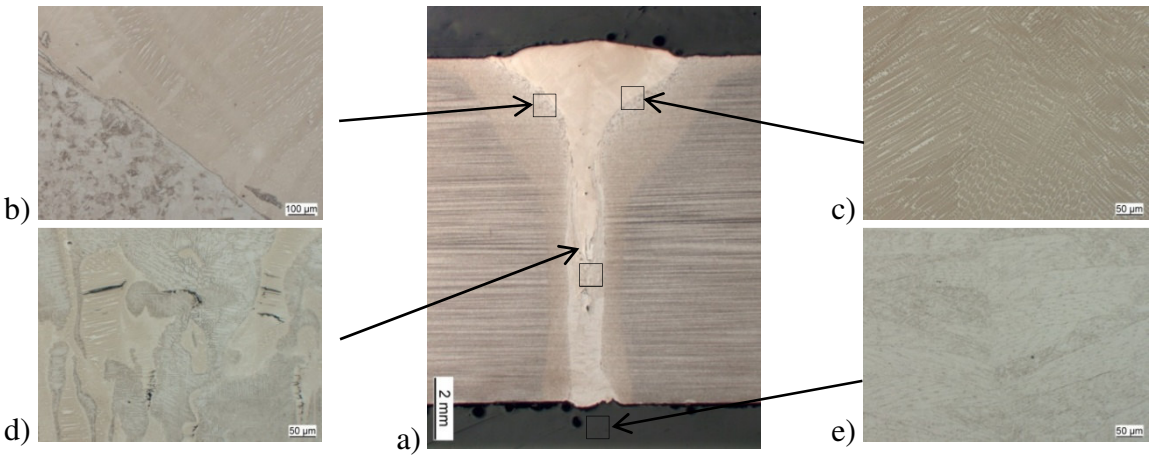

Figure 7 Hybrid laser-arc weld (P_{laser} = 13.8 kW, v_{weld} = 3.0 m/min, v_{wire} = 12 m/min, I = 330 A, U = 33 V), varying magnifications of the same weld with focus on the fusion boundary and FZ: general shape (a); top part (b, c); middle (d) and root part (e)

2.2 Distribution of filler wire in the FZ

In the welds performed with filler material EPMA has been done to obtain quantitative information about distribution of the alloying element Ni. The reason for such analysis is that alloying elements have a very direct influence on the mechanical properties of the weld joint. The key factors are adequate concentration and homogenous distribution through the FZ. Understanding these factors will help to optimize the welding process parameters for achieving required weld properties in particular impact toughness.

Figure 8 and Figure 9 show monochrome and color mapping of the Ni concentration profile in the cross section of a laser cold wire weld and a HLAW weld respectively. Results presented for laser cold wire weld show that distribution of filler material is very inhomogeneous starting from the weld upper surface. The average dilution of Ni near the upper surface is about 18%...20%. It is also evident that distribution of filler material is affected by the metal flow in the key hole. Parts of the molten filler material were carried by the melt flow to weld depths reaching ½ of the plate thickness. The maximum concentration was about 17% in the weld center at that depth. It can be interpreted from the color Ni mapping in Figure 8, that only a minor part of filler material reaches a depth of ½ of the plate thickness. The average dilution of Ni in the middle of plate thickness stays at 10%...11%. It is to worth noting that the filler material tends to accumulate along the fusion boundary to a depth of 9 to 10 mm from the top-side of the weld with a concentration of 13%...14% Ni in these thin regions. At the bottom near the root Ni concentration was about 9% which corresponds to the Ni content in the base material.

In general, it can be stated that filler material made up only a slight part of the FZ in the laser cold wire welds. One of the main reasons for this was the modest amount of filler wire that was fed into the weld pool. In other words an adequate welding wire feeding speed should be taken into account. At a filler wire speed of 2 m/min and welding speed of 2 m/min the fraction of the FZ compromised of the filler material was about 5.8% (Figure 8). This value was calculated by taking into consideration the actual geometrical shape of the FZ. A width of 1.7 mm, and a height of 11.5 mm was used in the calculations, along with 1.2 mm for the wire diameter. An increase of the wire feeding speed to 12 m/min would increase the fraction of filler material in the FZ to about 35%.

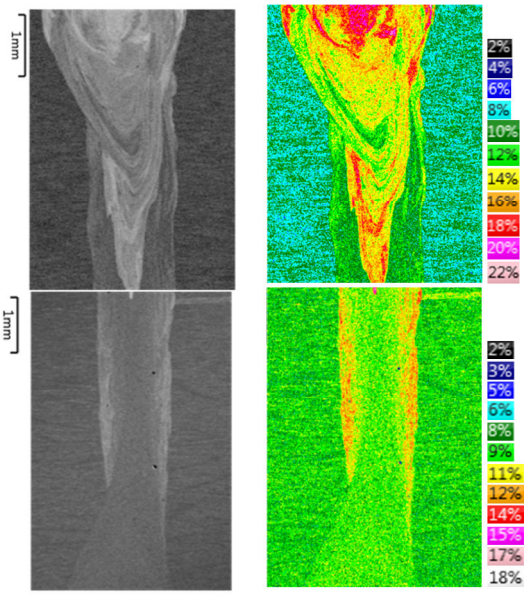

Figure 8 – Ni concentration profiles in cross section of the cold wire laser weld; monochrome profile (left) and color element map (right)

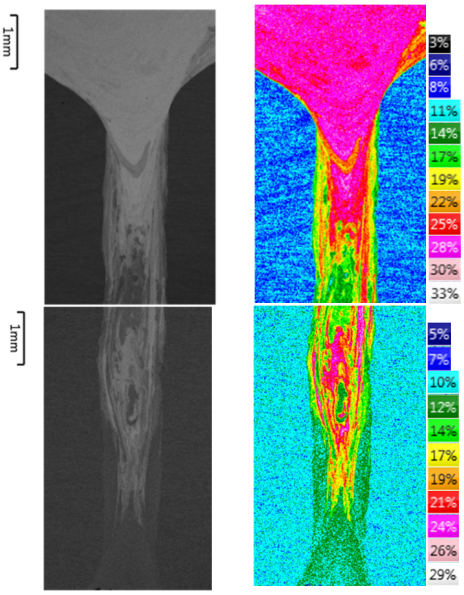

Figure 9 – Ni concentration profiles in cross section of the HLAW weld; monochrome profile (left) and color element map (right)

Based on the experience gained with respect to the laser cold wire welding process, it is proposed that wire feeding angle has to be 45° or more. Having the wire flatter to the specimen surface will help to avoid the stumbling of the wire tip against the cold welding pool edges and reach much higher wire feeding rates which is desirable for laser cold wire welding in LNG applications.

Wire feeding speeds of 12 m/min and higher are common for HLAW of thick walled constructions. Accordingly, it is expected that the mechanical properties of the weld can be positively influenced by a proper amount of filler material in the FZ. The uniform distribution of filler wire in the FZ is a necessary precondition. The measurements however show that the main volume of the filler material is concentrated in the top part of the weld in the arc dominated zone. The dilution here is homogeneous with the maximum concentration of Ni at about 30% (Figure 9). The mixing between the base and filler metal create Ni-poor and Ni-enriched “islands” which contain about 10% and 30% Ni respectively. These island like formations can be recognized as the inhomogeneous area, which starts from about 5 mm from the top side and reaches a depth of about 10 mm. It is remarkable that the filler material reaches the root side. The maximum Ni concentration here is about 12% which is 3% higher than Ni content is in base material.

The inhomogeneous mixing which is visible in the middle of the weld is undesirable, since it has areas with different physical properties such as thermal expansion. As a result, solidification cracks can occur in this area (Figure 7d).

The current state of results shows that further welding trials are necessary to achieve better homogeneity of weld metal in FZ. It is indicated in [13], that the HLAW process has a more homogeneous distribution of alloying elements with leading laser as compared to leading arc. In this research work it is also pointed out that almost homogeneous distribution of alloying elements can be attained when the shielding gas contained more than 2% O_2.

2.3 Hardness measurements and tensile tests

Hardness measurements HV0.5 and tensile tests were carried out to characterize the achieved mechanical properties of the welds. The Vickers hardness testing machines had been calibrated according to DIN EN ISO 6507-3. The maximum deviation of the hardness measurements HV0.5 was ±3%. The representative measuring results for the Vickers hardness for autogenous laser weld and HLAW are illustrated in Figure 10 and Figure 11 respectively.

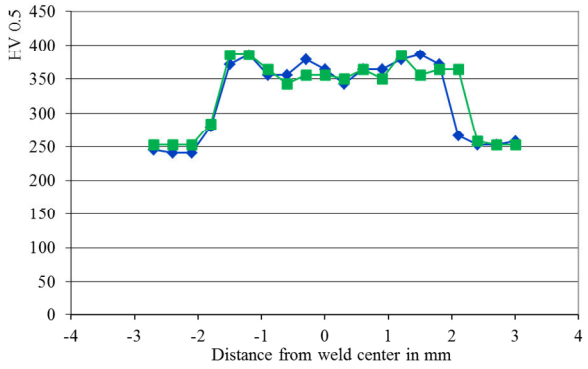

Figure 10 – The hardness HV0.5 profile for autogenous laser weld (blue is top side, green is root side)

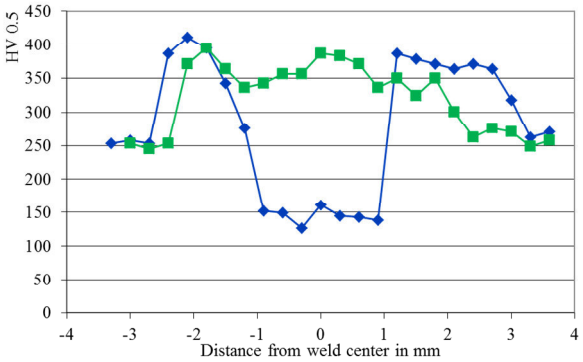

Figure 11 – The hardness HV0.5 profile for HLAW (blue is top side, green is root side)

The comparison shows that the peak hardness level for autogenous laser weld measured in both top and root side was 390 HV0.5 and exceeds the hardness of the base metal 250

HV0.5 by about 60% (Figure 10). This hardness level is quite high and can lead to reduced toughness of the weld joint at cryogenic temperatures. An unusual hardness profile can be observed at the laser hybrid weld (Figure 11). The hardness profile on the top side of the weld is characterized by the increased hardness in the HAZ from the base metal 250 HV0.5 up to 410 HV0.5 and then abruptly dropping down to 150 HV0.5 in the FZ. The drop in hardness of the top side FZ is explained by the high concentration of the Ni based filler material which is softer than the base metal. Only a nominal amount of filler material reaches the root side of the weld. Subsequently, the hardness level on the root side of the laser hybrid weld is high, similar to the autogenous laser weld.

Tensile tests were carried out according to DIN EN ISO 4136 using flat specimens at room temperature. Three specimens were tested for both laser welds and HLAW. The strength of the weld metal for all welds was always much higher than that of the base metal. The fracture location for all specimens tested was in the base metal (Figure 12).

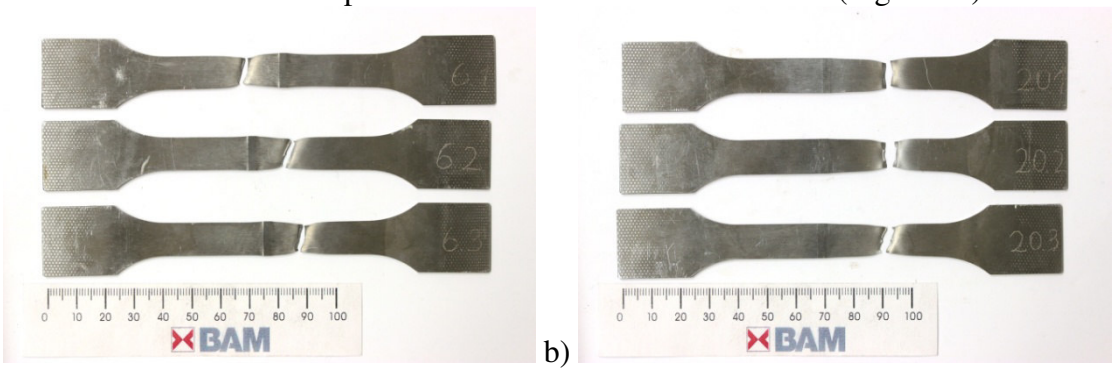

Figure 12 – Tensile test samples with fracture location in the base metal: autogenous laser weld (a); HLAW (b)

The average obtained failure stress was 768±2.5 MPa. The requirements of DIN EN 10028-4 for cryogenic steel X8Ni9 (Table 2) are definitely fulfilled with the obtained failure stresses.

In order to correlate the distribution of the filler wire in the weld to toughness, Charpy impact testing will be performed as the next step of this research work.

3. CONCLUSIONS

Plates made from cryogenic 9%Ni steel with thickness of 11.5 mm were butt joint welded in a single pass using three welding techniques; autogenous laser welding, laser cold wire welding and hybrid laser-arc welding process. The aim of these welding trials was to contribute to an understanding of how the welding process parameters affect the process stability, weld seam formation and mechanical properties of the welds. The findings of the study can be summarized as follows:

(1) A stable and reproducible welding process with a sound weld seam formation could be obtained for all three welding techniques tested, although the HLAW process needs an increased welding speed of about 3 m/min to avoid the droplet formation on the root side of the welds;

(2) The distribution of Ni base filler material is very inhomogeneous in laser cold wire welds starting from the weld upper surface. The element mapping shows that only a minor part of filler material reaches a depth of ½ of the plate thickness. No filler material could be detected at the bottom near the root of the laser cold wire welds;

(3) The homogenous distribution of the filler material up to weld depth of roughly 6 mm could be stated for the HLAW process. The Ni content of up to 30% is characteristically for this arc dominated part of the weld. The inhomogeneous

mixing between the Ni-poor and Ni-enriched formations with Ni content of about 10% and 30% respectively can be recognized in the plate middle. The maximum Ni concentration at the root side of the HLAW welds riches about 12% which is 3% higher than Ni content is in base material;

(4) The peak hardness for the laser welds was 390 HV0.5 and exceeds the hardness of the base metal by about 60%. This hardness level is quite high and can lead to reduced toughness of the weld joint at cryogenic temperatures. The hardness profile for HLAW welds variates from 410 HV0.5 to 150 HV0.5 depending on local distribution of the filler material through the cross section of the weld.

(5) The strength of the weld metal for both laser welds and HLAW welds was much higher than that of the base metal. The fracture location for all tested welds was in the base metal.

(6) The correlation between the distribution of the filler wire in the weld and the toughness will be examined by Charpy impact testing. The comparative Charpy tests at cryogenic temperature of 196°C will be done as the next step of this research work.

Acknowledgement

The welding experiments were carried out within the joint innovative project (support code of DLR Project Management Agency, Germany 01DH14012) between Central Metallurgical Research and Development Institute (CMRDI) of Egypt and Fraunhofer IPK of Germany. The project is supported by the Science and Technology Development Fund (STDF) of the Arab Republic of Egypt and the Federal Ministry of Education and Research (BMBF) of the Federal Republic of Germany.

REFERENCES

[1] “Liquefied Natural Gas: Understanding the Basic Facts”, August 2005, DOE/FE-0489. Available at: http://energy.gov/sites/prod/files/2013/04/f0/LNG_primerupd.pdf (in English)

[2] “World LNG Report – 2015 Edition”. Available at: http://www.igu.org/sites/default/files/node-page-field_file/IGU-World%20LNG%20Report-2015%20Edition.pdf (in English)

[3] R. Götz., „Der künftige Erdgasbedarf Europas“, Diskussionspapier. Available at: http://www.swp-berlin.org/fileadmin/contents/products/arbeitspapiere/Der_Erdgasbedarf_der_EU_11_05_1__ks.pdf , FG 5 2007/08, Mai 2007 (in German)

[4] J. Thierçault, C. Egels, “Cryogenic Above Ground Storage Tanks: Full Containment and Membrane Comparison of Technologies”, Proc. on “LNG 17 International Conference & Exhibition on Liquefied Natural Gas”, Houston, Texas, USA, 16-19 April 2013, ISBN 978-1-62993-533-1, pp. 122–130. (in English)

[5] Y.M. Yang, J.H. Kim, H.S Seo “Development Of The World’s Largest Above-Ground Full Containment LNG Storage Tank” , Proc. On “23rd World Gas Conference”, Amsterdam 2006, Korea Gas Corporation, Korea. (in English)

[6] M. Hoshino, et al., Development of Super-9%Ni Steel Plates with Superior Low-temperature Toughness for LNG Storage Tanks, Nippon Steel Technical Report, No. 90 (July 2004), pp. 20–24. (in English)

[7] Welding liquid natural gas tanks and vessels in 5% and 9% nickel steels. Available at: https://www-off-axis.fnal.gov/flare/technical_papers/welding_tanks.pdf (in English)

[8] Kobelco’s Welding Consumables for LNG Storage Tanks Made of 9% Ni Steel, KOBELCO Welding Today, Vol. 14 (2011), No. 2. (in English)

[9] Welding-based processing of nickel-alloyed steels for low temperature applications, Guidelines DVS 0955. (in English)

[10] R. Sakamoto, et al. "Development of Vertical Submerged Arc Welding Method for Aboveground LNG Storage Tank Construction." IHI Eng. Rev. 43.2 (2010): 55–62. (in English)

[11] S. Gook, A. Gumenyuk, and M. Rethmeier. "Hybrid laser arc welding of X80 and X120 steel grade." Science and Technology of Welding and Joining 19.1 (2014): 15–24. ISSN 1362-1718 (in English)

[12] M. Karhu, V. Kujanpää, A. Gumenyuk, M. Lammers, Study of Filler Metal Mixing and its

Implication on Weld Homogeneity of Laser-Hybrid and Laser Cold-Wire Welded Thick Austenitic Stainless Steel Joints, 32nd Int. Congress on Lasers and Electro-Optics (ICALEO2013), Oct. 6-10, 2013, Miami, FL, U.S.A., Paper ID: 906, pp. 252–261. (in English)

[13] L. Zhao, et al., Influence of Welding Parameters on distribution of Feeding Elements in CO_2 Laser GMA Hybrid Welding, Science and Technology of Welding and Joining (2009), Vol. 14, No. 5, pp. 457–467. (in English)

Laser and Hybrid Laser-Arc Welding of Cryogenic 9%NI Steel

S. Gook*[1], A. Gumenyuk*,[2], M. Rethmeier*,**[3], A.M. El-Batahgy***[4]**

** Fraunhofer Institute for Production Systems and Design Technology IPK, Pascalstraße 8-9, Berlin 10587*
[1]e-mail: sergej.gook@ipk.fraunhofer.de
*** Federal Institute for Materials Research and Testing BAM, Unter den Eichen 87 Berlin 12205*
[2]e-mail: andrey.gumenyuk@bam.de ; [3]e-mail: michael.rethmeier@bam.de
**** Central Metallurgical R&D Institute, Manufact Technology Dept., Helwan, P.O. Box 87, Helwan, Cairo, Egypt 11421*
[4]e-mail: elbatahgy@yahoo.comuring

Abstract – Heat treated 9%Ni steel is considered the most suitable and economic material for construction of large-size liquefied natural gas (LNG) storage tanks which operate at cryogenic temperatures (-196°C). Strength above 700 MPa as well as a minimum impact value of 60 J are required to ensure reliable operation of the LNG tanks at operating temperature. Conventional arc welding processes, including shielded metal arc welding, gas metal arc welding, gas tungsten arc welding and submerged arc welding, are currently used in construction of LNG tanks. Ni based filler wire is the preferred filler metal of choice in LNG tank construction. The main problem with this choice is the lower mechanical properties, particularly tensile strength of the weld metal. To compensate, the wall thickness needs to be excessively thick to ensure the strength of the welded structures. Ni based filler material is expensive and a large quantity is needed to fill the multi-pass weld grooves. These factors significantly add to the cost in the fabrication of LNG storage tanks. For these reasons, exploration of new welding technologies is a priority. A big potential can be seen in laser based welding techniques. Laser beam welding results in much smaller fusion zone with chemical composition and mechanical properties similar to that of the base material. Laser welding is a much faster process and allows for a joint geometry which requires less filler material and fewer welding passes. The advantages of laser welding can help to overcome the problems pointed out above.

Trials of autogenous laser welding, laser cold-wire welding and hybrid laser-arc welding conducted on the 9%Ni steel are presented in this paper. Chemical composition of the weld metal as well as effects of welding parameters on the weld formation, microstructure and tensile strength is discussed. Filler wire penetration depth as well as character of its distribution in the narrow laser welds was examined using EPMA - electron probe microanalysis.

*Keywords***:** cryogenic steel, laser welding, microstructure, hardness, tensile strength.